

Robust Ultrafast Currents in Molecular Wires through Stark Shifts

Ignacio Franco,¹ Moshe Shapiro,² and Paul Brumer¹

¹*Chemical Physics Theory Group, Department of Chemistry, and Center for Quantum Information and Quantum Control, University of Toronto, Toronto, Ontario, Canada*

²*Chemical Physics Department, The Weizmann Institute, Rehovot, Israel, and Departments of Chemistry and Physics, The University of British Columbia, Vancouver, British Columbia, Canada*
(Received 4 June 2007; published 17 September 2007)

A novel way to induce ultrafast currents in molecular wires using two incident laser frequencies, ω and 2ω , is demonstrated. The mechanism relies on Stark shifts, instead of near-resonance photon absorption, to transfer population to the excited states and exploits the temporal profile of the field to generate phase-controllable transport. Calculations in a *trans*-polyacetylene oligomer coupled to metallic leads indicate that the mechanism is highly efficient and robust to ultrafast electronic dephasing processes induced by vibronic couplings.

DOI: [10.1103/PhysRevLett.99.126802](https://doi.org/10.1103/PhysRevLett.99.126802)

PACS numbers: 85.65.+h, 72.10.Di, 73.63.-b, 78.20.Jq

Considerable effort has been devoted to studies of the properties of molecular wires [1] as the basic building blocks of nanoscale electronics. The focus is normally placed on the transport properties of metal-molecule-metal junctions subject to a bias voltage. In this regime, the metallic leads are the main source of electrons for the transport while the molecular system serves as a transporting medium that can be chemically functionalized to modify the I - V characteristics of the junction.

Here we consider an alternative situation in which the junction is not subject to a bias voltage and where the molecule serves as the main source of transporting electrons. The composite system is taken to be spatially symmetric and net currents are induced using lasers with frequency components ω and 2ω . Such fields give rise to phase-controllable transport in symmetric systems [2–4] even when they have a zero temporal mean. This rectification effect first appears in the third order response of the system to the incident radiation [4]. The setup is of interest in molecular wires since it can produce ultrafast currents and could lead to the development of molecular switches that operate on a femtosecond time scale.

In the usual way that the scenario is applied, the frequencies of the $\omega + 2\omega$ field are chosen at or near resonance. The resulting multiphoton absorption processes serve the double purpose of creating laser-induced rectification and transferring population to transporting states. Such a setup, however, is fragile to decoherence processes since it relies on creating coherent superposition states [2]. This aspect becomes particularly troublesome when applying the scenario to molecular nanojunctions as most molecules exhibit strong electron-vibrational couplings [1,5] that introduce ultrafast coherence loss (in less than 10 fs [6]) and internal relaxation mechanisms in the electronic dynamics [7].

In fact, recent calculations [7] show that vibronic couplings can make the laser rectification in molecular wires extremely inefficient. In that study we found that less than

4% of the photoexcited electrons participated in the current, whereas equivalent but rigid systems exhibited 60% efficiencies. Hence, in order to generate sizable currents considerable energy from the laser field needs to be dumped into the nanojunction compromising its structural integrity. Further, employing faster or stronger pulses is not very helpful [7] since they introduce other satellite channels in the control and do not appreciably overcome the deleterious effects of the vibronic couplings.

In this Letter we present an alternative mechanism that is remarkably robust to electron-vibrational couplings, survives in the presence of decoherence and thermal effects, and is able to induce large currents in molecular wires with efficiencies $>90\%$. Instead of promoting electrons to the conduction band through absorption of photons, we work far off resonance and employ Stark shifts to nonadiabatically couple the ground and excited electronic states. Phase-controllable symmetry breaking is achieved by exploiting the difference in the intensity of $\omega + 2\omega$ fields for positive and negative amplitudes.

As a system we consider a *trans*-polyacetylene (PA) oligomer connected by its ends to macroscopic metallic leads. The leads are treated as rigid semi-infinite tight-binding chains while the oligomer is described using the well-known Su-Schrieffer-Heeger (SSH) Hamiltonian [8]. The SSH model treats the molecule as a tight-binding chain in which the π electrons are coupled to distortions in the polymer backbone by electron-vibrational interactions. It is remarkably successful in reproducing the electronic structure and dynamics of excitations of PA.

The photoinduced electron-vibrational dynamics of the nanojunction is followed in a mean-field (Ehrenfest) mixed quantum-classical approximation where transitions between instantaneous eigenstates are allowed [9]. The effect of lattice fluctuations is incorporated by propagating an ensemble of quantum-classical trajectories with initial conditions selected from the ground-state nuclear Wigner distribution function of the chain. In this way the dynamics

reflects the initial nuclear quantum distribution and is subject to the level broadening and internal relaxation mechanism introduced by the vibronic couplings in the wire [7]. We have found that this method describes the trends observed in a recent sub-10 fs experiment performed on PA [10]. In addition, we introduce projective lead-molecule couplings so that basic aspects of the Fermi sea are taken into account without explicitly following the dynamics of the essentially infinite number of particles in the leads.

The nanojunction is described as a one-dimensional lattice in which each site n corresponds to the position of an atom, and is defined by the Hamiltonian

$$H(t) = H_L + H_{S-L} + H_S(t) + H_{S-R} + H_R. \quad (1)$$

Here $H_L = -t_{\text{lead}} \sum_{n < 0, s} c_{n+1, s}^\dagger c_{n, s} + \text{H.c.}$ and $H_R = -t_{\text{lead}} \sum_{n > N, s} c_{n+1, s}^\dagger c_{n, s} + \text{H.c.}$ describe the left (L) and right (R) lead with hopping parameter t_{lead} . The operator $c_{n, s}^\dagger$ ($c_{n, s}$) creates (annihilates) a fermion in site n and spin s , and H.c. denotes the Hermitian conjugate. The SSH oligomer with Hamiltonian $H_S(t) = H_{\text{el}} + H_{\text{latt}}$ is situated between sites $n = 1, \dots, N$ and is coupled to an electric field $E(t)$ in the dipole approximation. Specifically, the electronic part of H_S is

$$H_{\text{el}} = \sum_{n=1, s}^{N-1} [-t_0 + \alpha(u_{n+1} - u_n)](c_{n+1, s}^\dagger c_{n, s} + c_{n, s}^\dagger c_{n+1, s}) + |e| \sum_{n=1, s}^N x_n c_{n, s}^\dagger c_{n, s} E(t), \quad (2)$$

where t_0 is the hopping integral for zero displacement, u_n is the monomer displacement of site n , and α describes the electron-ion coupling between neighboring sites. In turn, $x_n = (na + u_n)$ is the position operator for site n , a the lattice constant, and $-|e|$ the unit electronic charge. The lattice is described by

$$H_{\text{latt}} = \frac{M}{2} \sum_{n=1}^N \dot{u}_n^2 + \frac{K}{2} \sum_{n=1}^{N-1} (u_{n+1} - u_n)^2 - |e| \sum_{n=1}^N x_n E(t), \quad (3)$$

with force constant K and (CH) group mass M .

We consider the case where no bias voltage is applied across the bridge and focus on the short time dynamics of the system. In this regime, the basic function of the leads is to absorb electrons from the molecule with energy higher than the Fermi energy ϵ_F , taken to be the zero-reference energy, and to block them otherwise. We focus on electronic transport and model this effective coupling using projection operators. Specifically, the lead-molecule coupling

$$H_{S-L}(t) = -t_{\text{coup}} \sum_{n \in S, s} \mathcal{P}_{1, n}^S(t) c_{0, s}^\dagger c_{n, s} + \text{H.c.}, \quad (4)$$

$$H_{S-R}(t) = -t_{\text{coup}} \sum_{n \in S, s} \mathcal{P}_{N, n}^S(t) c_{N+1, s}^\dagger c_{n, s} + \text{H.c.},$$

is a restricted tight-binding interaction with coupling constant t_{coup} in which only electrons with energy $\epsilon_\gamma > \epsilon_F$ are deposited in the contacts. Here

$$\mathcal{P}^S(t) = \sum_{\epsilon_\gamma > \epsilon_F} |\gamma_S(t)\rangle \langle \gamma_S(t)|$$

projects into the instantaneous molecular π^* light-dressed eigenorbitals defined by the eigenvalue relation $H_{\text{el}}(t)|\gamma_S(t)\rangle = \epsilon_\gamma |\gamma_S(t)\rangle$, and $\mathcal{P}_{n, m}^S = \langle n | \mathcal{P}^S | m \rangle$ with $|n\rangle = c_{n, s}^\dagger |0\rangle$ where $|0\rangle$ is the vacuum state. Note that since the SSH model is electron-hole symmetric a subsequent inclusion of hole transport is just expected to double the resulting current.

In the mean-field approximation [9] the nuclei are described by classical trajectories determined by

$$M\ddot{u}_n = -\langle \Psi(t) | \frac{\partial H(t)}{\partial u_n} | \Psi(t) \rangle = -K(2u_n - u_{n+1} - u_{n-1}) + 2\alpha \text{Re}\{\rho_{n, n+1} - \rho_{n, n-1}\} - |e| E(t)(\rho_{n, n} - 1). \quad (5)$$

Here $\rho_{n, m} = \sum_s \langle \Psi(t) | c_{n, s}^\dagger c_{m, s} | \Psi(t) \rangle = \sum_{\epsilon, s} f(\epsilon, s) \langle m | \epsilon(t) \rangle \langle \epsilon(t) | n \rangle$ is the electronic reduced density matrix, and $f(\epsilon, s)$ is the time-independent initial distribution function (that takes values 0 or 1 depending on the occupation of each level with energy ϵ and spin s). We take the chain to be clamped, so that $u_1(t) = u_N(t) = 0$ at all times. In turn, the orbitals $|\epsilon(t)\rangle$ that form the \mathcal{N} -electron wave function $|\Psi(t)\rangle$ satisfy the time-dependent Schrödinger equation

$$i\hbar \frac{d}{dt} \begin{bmatrix} |\epsilon_L(t)\rangle \\ |\epsilon_S(t)\rangle \\ |\epsilon_R(t)\rangle \end{bmatrix} = \begin{bmatrix} H_L & H_{S-L}(t) & 0 \\ H_{S-L}(t) & H_{\text{el}}(t) & H_{S-R}(t) \\ 0 & H_{S-R}(t) & H_R \end{bmatrix} \begin{bmatrix} |\epsilon_L(t)\rangle \\ |\epsilon_S(t)\rangle \\ |\epsilon_R(t)\rangle \end{bmatrix},$$

where $|\epsilon_P\rangle = \sum_{n \in P} \langle n | \epsilon \rangle |n\rangle$ describes the part of the orbital in region $P = L, R$, or S . We take the leads and molecule to be initially detached and, since the projective coupling [Eq. (4)] already incorporates the Fermi blockade imposed by the leads, only consider orbitals that are initially in the molecular region, so that $|\epsilon_\beta(0)\rangle = 0$ with $\beta = L$ or R .

As the composite system is spatially unbounded, it is necessary to obtain an equation of motion for the system part of the orbitals $|\epsilon_S\rangle$ where we do not need to explicitly follow its behavior in the lead regions. This can be accomplished by applying Laplace transform techniques to the evolution equation for the lead components, to obtain $|\epsilon_\beta(t)\rangle = (1/i\hbar) \int_0^t U^\beta(t - \tau) H_{S-\beta}(\tau) |\epsilon_S(\tau)\rangle d\tau$. Here the evolution operator for the isolated leads $U^\beta(t) = \exp(-iH_\beta t/\hbar)$ acts as the memory kernel of the convolution integral. Its matrix elements in site representation can be determined in closed form. For this, note that H_β is diagonalized by the basis transformation $c_{n, s} = (2/\mathcal{M})^{1/2} \sum_{k=1}^{\mathcal{M}} \sin[(n - n_\beta)k\pi/\mathcal{M}] c_{k, s}$, where \mathcal{M} is the number of lead sites, $n_L = 1$, and $n_R = N$. It then follows

that $U_{n,m}^\beta(t) = i^{n-m} J_{n-m}[(2t_{\text{lead}}/\hbar)t] - i^{n+m-2n_\beta} J_{n+m-2n_\beta}[(2t_{\text{lead}}/\hbar)t]$ for large \mathcal{M} , where $J_n(z) = (i^{-n}/\pi) \times \int_0^\pi e^{iz \cos \theta} \cos(n\theta) d\theta$ is a Bessel function of the first kind of order n . Hence,

$$i\hbar \frac{\partial}{\partial t} \langle n | \epsilon_S(t) \rangle = \langle n | H_{\text{el}}(t) | \epsilon_S(t) \rangle + \frac{t_{\text{coup}}^2}{i\hbar} \sum_{m=1}^N \int_0^t \mathcal{K}(t-\tau) \Gamma_{n,m}(t, \tau) \langle m | \epsilon_S(\tau) \rangle d\tau, \quad (6)$$

where $\Gamma_{n,m}(t, \tau) = \mathcal{P}_{n,1}^S(t) \mathcal{P}_{1,m}^S(\tau) + \mathcal{P}_{n,N}^S(t) \mathcal{P}_{N,m}^S(\tau)$. Equation (6) is an effective non-Markovian Schrödinger equation for the system part of the orbitals. The first term corresponds to the single-particle Schrödinger equation for the isolated system. The convolution integral with memory kernel $\mathcal{K}(t) = U_{0,0}^L(t) = U_{N+1,N+1}^R(t) = 2J_1[(2t_{\text{lead}}/\hbar)t]/(2t_{\text{lead}}/\hbar)t$ describes the transfer of population from the system into the leads.

We now invoke the wide bandwidth approximation, where $\hbar/2t_{\text{lead}}$ becomes the fastest time scale in the problem. In this regime, Eq. (6) reduces to its Markovian limit

$$i\hbar \frac{\partial}{\partial t} \langle n | \epsilon_S \rangle = \sum_{m=1}^N \left[\langle n | H_{\text{el}}(t) | m \rangle - i \frac{t_{\text{coup}}^2}{t_{\text{lead}}} \Gamma'_{n,m}(t) \right] \langle m | \epsilon_S \rangle, \quad (7)$$

and the leads are effectively mapped into a negative imaginary (absorbing) potential. The projection operators in the coupling, contained within $\Gamma'_{n,m}(t) = \Gamma_{n,m}(t, t)$, ensure that only those electrons with sufficient energy get absorbed with proper conservation of the antisymmetry principle. The equation is valid for times $t \gg \hbar/t_{\text{lead}}$, but it can be used for all times by slowly turning on the lead-molecule interaction, a strategy that we adopt. Note that the field influences the dynamics directly by inducing transitions among states, and indirectly by modifying the wire-lead couplings. Equations (5) and (7) constitute a closed set of $N(N+2)$ first-order differential equations that are integrated using a Runge-Kutta method of order 8. The projective term in the dynamics $\Gamma'_{n,m}(t)$ is updated at every time step by diagonalizing $H_{\text{el}}(t)$. Throughout we use the standard SSH parameters [8]: $\alpha = 4.1 \text{ eV/\AA}$, $K = 21 \text{ eV/\AA}^2$, $t_0 = 2.5 \text{ eV}$, $M = 1349.14 \text{ eV fs}^2/\text{\AA}^2$, and $a = 1.22 \text{ \AA}$. In turn, we take the molecule and leads to be weakly coupled with $t_{\text{coup}}^2/t_{\text{lead}} = 0.1 \text{ eV}$.

Electronic dephasing due to vibronic coupling is incorporated by integrating the equations for an ensemble of 1000 initial conditions. The initial conditions are generated using the following strategy [7]: the starting optimal geometry is obtained by minimizing the total ground-state energy of the chain. Then, a normal mode analysis around this geometry is performed, yielding the ground-state nuclear Wigner phase space distribution function $\rho_W(\mathbf{u}, \mathbf{p})$ in the harmonic approximation, where $\mathbf{u} = (u_1, \dots, u_N)$ and $\mathbf{p} = M(\dot{u}_1, \dots, \dot{u}_N)$. By importance sampling this distribution an ensemble of lattice initial conditions $\{\mathbf{u}^i(0), \mathbf{p}^i(0)\}$ is generated. The associated initial values for the orbitals $\{|\epsilon^i(0)\rangle\}$ are obtained by diagonalizing H_{el} for each initial geometry of the lattice $\{\mathbf{u}^i(0)\}$. Each member i of the ensemble defines a quantum-classical trajectory

$(\mathbf{u}^i(0), \mathbf{p}^i(0), |\Psi^i(0)\rangle) \rightarrow (\mathbf{u}^i(t), \mathbf{p}^i(t), |\Psi^i(t)\rangle)$ and the set is used to obtain ensemble averages. We note that the resulting initial state is basically stationary under field-free evolution.

The current entering into lead β is defined by $j_\beta = -|e| \partial p_\beta / \partial t$, where $p_\beta = \sum_{n \in \beta} p_{n,n}$ is the number of electrons in lead β . Using the same set of techniques employed to arrive at Eq. (7), one can obtain an equation for $j_\beta(t)$ that solely depends on molecular properties: $j_\beta(t) = -(2|e|/\hbar) (t_{\text{coup}}^2/t_{\text{lead}}) \sum_{m,n} \text{Re}\{\mathcal{P}_{n_\beta,m}^S(t) \mathcal{P}_{n,n_\beta}^S(t) \rho_{n,m}(t)\}$. Any rectification generated by $\omega + 2\omega$ pulses manifests as $j_L - j_R \neq 0$.

We study neutral 100-site chains initially in the ground electron-vibrational state. The geometry of the chain consists of a perfect alternation of double and single bonds. The electronic structure is composed of 50 doubly occupied valence π orbitals and 50 empty π^* states, separated by an energy gap of $2\Delta = 1.3 \text{ eV}$. We follow the electron-vibrational dynamics of the wire under the influence of an $\omega + 2\omega$ field of the form

$$E(t) = \epsilon_\omega \cos(\omega t + \phi_\omega) + \epsilon_{2\omega} \cos(2\omega t + \phi_{2\omega}). \quad (8)$$

The field is smoothly turned on and off in 100 fs and has constant amplitude for 400 fs. The frequency $\hbar\omega = 0.2\Delta$ is chosen far off resonance from the system's interband transition frequencies so that Stark shifts, and not photon absorption, dominate the dynamics. The field amplitude used is $\epsilon_{2\omega} = 6.1 \times 10^{-3} \text{ V \AA}^{-1}$ with $\epsilon_\omega = 2\epsilon_{2\omega}$, which corresponds to an intensity $I_{2\omega} \sim 5 \times 10^8 \text{ W cm}^{-2}$.

Figure 1 shows the field, the currents, and electronic structure of the chain, averaged over all trajectories, when the relative phase of the pulse is $\phi_{2\omega} - 2\phi_\omega = 0$. The single-particle spectrum displays considerable Stark shifts and the field effectively reduces the energy gap of the oligomer, causing frequent crossings between the ground and excited electronic states in individual trajectories. Since the wire's ground state is nondegenerate and of definite parity, the lowest order contributions to the Stark effect is quadratic in the field. Hence, when $|E(t)|$ is maximum the energy gap acquires its minimum value. At the crossing times population is transferred from the valence to the conduction band and bursts of charge are deposited in the leads.

Note that for $\phi_{2\omega} - 2\phi_\omega = 0$ almost all excited electrons are deposited in the right contact only. Symmetry breaking arises due to the difference in the maximum $|E(t)|$ for positive and negative field amplitudes. Even when $E(t)$ has a zero temporal mean, it consists of narrow peaks with large $|E(t)|$ for positive amplitudes, and shallow and broad features when $E(t)$ is negative [Fig. 1(a)]. For this reason,

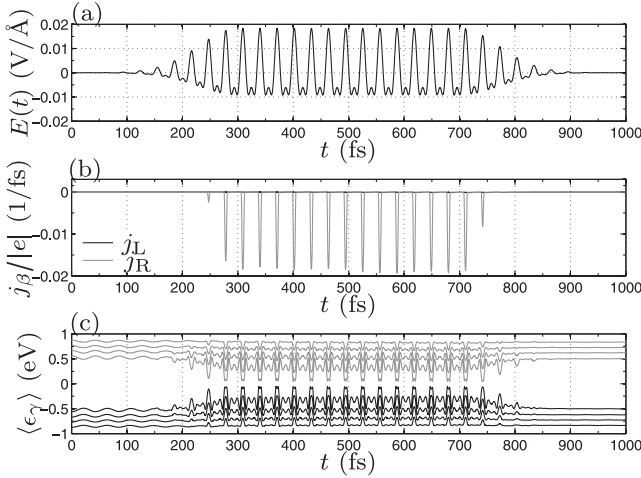


FIG. 1. Time dependence of (a) the electric field, (b) the current entering the left and right leads, and (c) the instantaneous field-dressed orbital energies for states near the energy gap for a 100-site flexible wire under the influence of the field in Eq. (8) with $\phi_{2\omega} - 2\phi_{\omega} = 0$. Note the bursts of charge deposited in the right lead when the field bridges the energy gap. Here j_L is so small that it is barely visible.

the Stark effect is only sufficiently strong to close the energy gap when the field has a positive amplitude. Thus, transfer of population to the conduction band and absorption of electrons by the leads always occurs when the laser is pointing at a particular and the same direction, in this way inducing directed transport in the system.

The phenomenon depends intimately on the relative phase. For instance, for the case of $\phi_{2\omega} - 2\phi_{\omega} = \pi/2$ (not shown) the electric field exhibits equal intensity for positive and negative amplitudes. Since the field changes sign between consecutive interband couplings, the bursts of charge deposited alternate between the left and right contact, and no net current is produced.

Figure 2 shows the net difference in charge deposited in the left and right leads after the pulse is over for different laser phases, as well as the efficiency of the process. For comparison purposes the plot also includes results obtained in an equivalent but rigid system. The system is made rigid by increasing the mass of the (CH) groups by 10^6 . We first note that the mechanism is robust to decoherence effects due to coupling to the vibrational degrees of freedom as well as satellite contributions due to parasite multiphoton absorption. In fact, 90% of the excited electrons can participate in the net current. Further, the sign and magnitude of the effect can be manipulated by varying the laser phases. By changing the relative phase by π the magnitude of the effect stays the same but the direction of the rectification is reversed.

In the flexible wire the rectification exhibits an almost sinusoidal dependence on $\phi_{2\omega} - 2\phi_{\omega}$. By contrast, in rigid wires for certain range of phases no currents are induced since the maximum field amplitude is not large

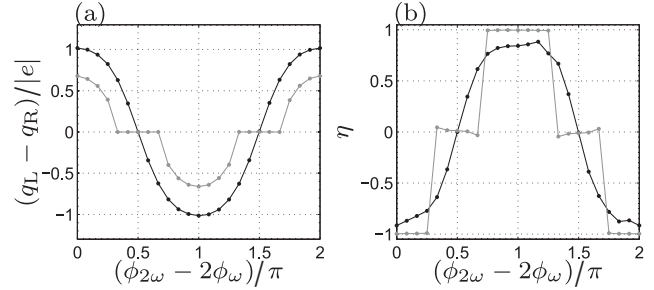


FIG. 2. Phase dependence of (a) the net rectification $q_L - q_R$, where $q_{\beta} = \int_0^t j_{\beta}(t)dt$ and (b) efficiency $\eta = (q_L - q_R)/(q_L + q_R)$ of the process when field (8) is applied to flexible (black dots) and rigid (gray dots) 100-site wires. Note the assistance of phonons in the rectification.

enough to couple valence and conduction bands. Hence, in this range the currents observed in the flexible wire are phonon assisted; i.e., the level broadening introduced by the vibrations permits the nonadiabatic coupling. The currents generated in the flexible case are always larger than in the rigid example. However, in rigid wires the mechanism can exhibit perfect efficiencies.

In conclusion, we have demonstrated a way to efficiently induce phase-controllable transport along molecular wires on a femtosecond time scale using $\omega + 2\omega$ fields. The effect employs Stark shifts to transfer population to transporting states and exploits the difference in the instantaneous field intensity for positive and negative amplitudes to generate rectification. It is robust to electron-vibrational couplings and other decoherence mechanisms, and is best suited for long oligomers.

-
- [1] C. Joachim and M.A. Ratner, Proc. Natl. Acad. Sci. U.S.A. **102**, 8801 (2005); A. Nitzan and M.A. Ratner, Science **300**, 1384 (2003); D.M. Adams *et al.*, J. Phys. Chem. B **107**, 6668 (2003); A. Salomon *et al.*, Adv. Mater. **15**, 1881 (2003).
 - [2] M. Shapiro and P. Brumer, *Principles of the Quantum Control of Molecular Processes* (Wiley, New York, 2003).
 - [3] G. Kurizki, M. Shapiro, and P. Brumer, Phys. Rev. B **39**, 3435 (1989); Y.Y. Yin *et al.*, Phys. Rev. Lett. **69**, 2353 (1992); E. Dupont *et al.*, Phys. Rev. Lett. **74**, 3596 (1995); A. Haché *et al.*, Phys. Rev. Lett. **78**, 306 (1997); M. Schiavoni *et al.*, Phys. Rev. Lett. **90**, 094101 (2003).
 - [4] I. Franco and P. Brumer, Phys. Rev. Lett. **97**, 040402 (2006).
 - [5] S. Tretiak *et al.*, Phys. Rev. Lett. **89**, 097402 (2002).
 - [6] H. Hwang and P.J. Rossky, J. Phys. Chem. B **108**, 6723 (2004).
 - [7] I. Franco, Ph.D. thesis, University of Toronto, 2007.
 - [8] A.J. Heeger *et al.*, Rev. Mod. Phys. **60**, 781 (1988).
 - [9] H.W. Streitwolf, Phys. Rev. B **58**, 14356 (1998).
 - [10] S. Adachi, V.M. Kobryanskii, and T. Kobayashi, Phys. Rev. Lett. **89**, 027401 (2002).